Toxicology Reports 8 (2021) 1937–1947

Contents lists available at ScienceDirect

Toxicology Reports

journal homepage: www.elsevier.com/locate/toxrep

Carbonic anhydrase inhibitor induces otic hair cell apoptosis via an intrinsic pathway and ER stress in zebrafish larvae

Hiroko Matsumoto [a], Hisako Miyagi [b], Nobuhiro Nakamura [b], Yasuhiro Shiga [a], Toshihiro Ohta [a], Shoko Fujiwara [a,*], Mikio Tsuzuki [a]

[a] School of Life Sciences, Tokyo University of Pharmacy and Life Sciences, Horinouchi, Hachioji, Tokyo, 192-0392, Japan
[b] Department of Life Science and Technology, Tokyo Institute of Technology, 4259-B13 Nagatsuta-cho, Midori-ku, Yokohama, 226-8501, Japan

ARTICLE INFO

Handling Editor: Dr. Aristidis Tsatsakis

Keywords:
Zebrafish
Carbonic anhydrase
Ethoxyzolamide
Hair cell
Neuromast
Apoptosis

ABSTRACT

Carbonic anhydrase (CA) catalyzes reversible hydration of CO_2 to HCO_3^- to mediate pH and ion homeostasis. Some chemical pollutants have been reported to have inhibitory effects on fish CA. In this study, we investigated effects of a CA inhibitor ethoxyzolamide (EZA) on neuromasts development during zebrafish embryogenesis, since embryogenesis in aquatic organisms can be particularly sensitive to water pollution. EZA caused alteration of pH and calcium concentration and production of reactive oxygen species (ROS) in larvae, and induced apoptosis in hair cells especially in the otic neuromast, in which CA2 was distributed on the body surface. mRNA levels of apoptotic genes and caspase activities were increased by EZA, whereas anti-oxidants and apoptotic inhibitors, Bax, NF-κB, and p53 inhibitors significantly relieved the induction of hair cell death. Also, mRNA levels of Bip and CHOP, which are induced in response to ER stress, were upregulated by EZA, suggesting that EZA induces otic hair cell apoptosis via the intrinsic mitochondrial pathway and ER stress. Our results demonstrated an essential role of CA in neuromast development via maintenance of ion transport and pH, and that the CA, which is directly exposed to the ambient water, shows marked sensitivity to EZA.

1. Introduction

Carbonic anhydrase (CA, EC 4.2.1.1.) catalyzes reversible hydration of CO_2 to bicarbonate (HCO_3^-) in various processes, including pH regulation, inorganic carbon (CO_2 and HCO_3^-) and ion transport, and maintenance of the hydroelectrolytic balance, in bacteria, plants and animals [1,2]. Some heavy metals, pharmaceuticals, and agrichemicals, which are recognized as important emerging environmental contaminants, were reported to have inhibitory effects on CA [3–7]. Thus, there are growing concerns about ecotoxicity of these CA inhibitors [8–11].

Zebrafish (*Danio rerio*) has recently emerged as a promising vertebrate model to evaluate the toxicity of chemical compounds, including drug candidates [12]. The zebrafish system has been applied to the assessment of novel CA inhibitors (anticancer inhibitors of CA IX [13,14], inhibitors of *Mycobacterium tuberculosis* β-carbonic anhydrase [15]). Some studies showed that CAs in gills and lateral line neuromasts located on the body surface show marked sensitivity to CA inhibitors, because these organs are directly exposed to the ambient environment and are critical for maintaining body fluid homeostasis [16,17].

Our previous study demonstrated that a cytosolic isoform, CA2 (previously termed CA2a), and a membrane-bound isoform, CA15a, are localized in hair cells and in the apical region of epithelial cells in the inner ear at the beginning of zebrafish embryogenesis, respectively [5]. It has been suggested that these CA isoforms play a central role in the transport of calcium, protons and bicarbonate ions, and thereby in optimal pH regulation and fluid homeostasis in the inner ear [18,19]. Also, loss of function of anion exchanger 1 (AE1) and Cl^-/HCO_3^- exchanger, which are major regulators of intracellular pH, leads to acidification of the endolymph in the inner ear and hair cell death in neuromasts [20].

Hair cells are present not only in the inner ear but also in neuromasts of the lateral line system, these cells being morphologically and functionally similar to each other. Thus, we assumed that CA also plays a significant role in the formation of neuromasts, and investigated the molecular mechanism of EZA-induced hair cell death, measuring changes in pH, the reactive oxygen species (ROS) and calcium levels,

Abbreviations: CA, carbonic anhydrase; EZA, ethoxyzolamide; dpf, days post-fertilization; PBS, phosphate-buffered saline.

* Corresponding author at: School of Life Sciences, Tokyo University of Pharmacy and Life Sciences, 1432-1 Horinouchi, Hachioji, Tokyo, 192-0392, Japan.
E-mail address: fujiwara@toyaku.ac.jp (S. Fujiwara).

https://doi.org/10.1016/j.toxrep.2021.11.018
Received 4 September 2021; Received in revised form 22 November 2021; Accepted 24 November 2021
Available online 26 November 2021

and the mRNA levels of apoptotic genes and caspase activities. Our results demonstrated that EZA effectively induces the intrinsic pathway of apoptosis through caspase activation and ER stress, via generation of ROS.

2. Materials and methods

2.1. Experimental animals

Zebrafish (RIKEN WT), which were kindly provided by RIKEN NBRP, were maintained as previously descrived [5]. Fertilized eggs were collected during the early hours of the morning and incubated in 0.3×Danieau's solution [21] at 28 °C until they were used in the experiments [5].

2.2. Drug treatment of embryos

Normally developing larvae at 6 h post-fertilization were selected, and treated with EZA (Sigma-Aldrich, USA) and its solvent, DMSO [0.1 % (v/v)]-containing 0.3×Danieau's solution. For the control group, DMSO [final concentration, 0.1 %(v/v)] was added. For observation of the effect of Ca^{2+} on EZA-induced hair cell death, high calcium medium containing $CaCl_2$ (Fujifilm Wako Pure Chemical Corporation, Japan) at five times the normal concentration was used [final concentration, 0.9 mM].

To assess the roles of anti-oxidants and apoptotic inhibitors in EZA-induced hair cell death, the following drugs were used together with 80 ppb (310 nM) EZA from 6 h to 3 days post-fertilization (dpf). Each agent, which had been dissolved in DMSO in advance, was diluted to a final concentration of 0.1 % DMSO (v/v) with 0.3×Danieau's solution, and was used at the optimum concentration that affected hair cell death without causing morphological changes.

Anti-oxidants included glutathione (GSH: 40 μM; Sigma-Aldrich, USA), allopurinol (ALO: 1 mM; Sigma-Aldrich, USA), D-methionine (MET: 100 μM; Sigma-Aldrich, USA). Buthionine sulfoximine (BSO:1mM; Sigma-Aldrich, USA), which is a pro-oxidant, was used as a negative control.

Apoptotic inhibitors included Bay 11-7085 (400 μM; Tokyo Chemical Industry, Japan), SN-50 (1 mM; Fujifilm Wako Pure Chemical Corporation, Japan), (±)-1-(3,6-dibromocarbazol-9-yl)-3-piperazin-1-yl-propan-2-ol (Bax inhibitor: 1 mM; Abcam, Japan), and Pifithrin-α (PIF-α: 1 mM; Sigma-Aldrich, USA).

For morphological assessment, after exposure to various concentrations of EZA from 6 h to 3 dpf, embryos in which some lesions and mortality were observed were recorded, as described previously [5].

2.3. Carbonic anhydrase assay

CA activity of zebrafish larvae that had been treated with 0.3, 1.3, 5, 20, 80, 310, and 1240 ppb (1.2, 4.8, 19, 77, 310, 1200, 5000 nM) EZA for 3 days was measured as previously described [5]. For each treatment, three replicates of forty larvae (about 10 μL) were washed three times and homogenized in 0.3×Danieau's solution (about 510 μL). To 20 μL of the resulting cytosol fraction, 80 μL of distilled water was added, and then bubbled with CO_2. To initiate the reaction, 100 μL of imidazole buffer (20 mM imidazole, 5 mM Tris, 0.2 mM p-nitro-phenol, pH 9.5) was added to the solution, and CA activity was determined spectrophotometrically at 410 nm. The activity was expressed as a percentage of the control.

2.4. Staining of hair cells in neuromasts

Neuromast hair cells in zebrafish larvae were labeled with fluorescent dye YO-PRO-1 (Thermo Fisher Scientific, USA), which can stain cellular nuclei by binding to DNA. Zebrafish larvae (four replicates, three larvae each) were incubated in 0.3×Danieau's solution containing 3 μM YO-PRO-1 for 15 min, rinsed three times with 0.3×Danieau's solution, and then anesthetized with 0.001 % buffered MS-222. The labeled hair cells in otic neuromasts were observed under a Leica DM2500 microscope with a green fluorescence filter set and an Olympus DP10 camera.

2.5. Morpholino-oligonucleotides injection

Antisense morpholino-oligonucleotides (MO) specific for CA2 (approximately 3 ng) in 1× Danieau's solution were injected into the yolk of one-cell embryos [22].

2.6. Immunohistochemical analysis

To examine the localization of CA2, zebrafish larvae at 1, 3, 5 dpf were overanesthetized, fixed in 10 % neutral buffered formalin and then embedded in paraffin. Tissue sections were de-paraffined and boiled for 20 min in a 1 mM EDTA (pH 9.0) solution by means of microwaving. Subsequently, the sections were immersed in methanol containing 0.5 % H_2O_2 for 30 min at room temperature to inhibit endogenous peroxidase activity, and then, blocked with 1% goat serum in PBS containing 0.25 % Triton (PBST) to prevent the non-specific binding of the antiserum. The sections were washed several times with PBST and incubated with rabbit-CA2 antibody (diluted 1:1,000) for 30 min at room temperature. After incubation, the antibody was visualized by using a Vectastain Elite ABC kit (Vector Laboratories, USA) and a Vector SG peroxidase substrate kit (Vector Laboratories, USA). After dehydration, the slides were mounted with Entellan new (Merck Millipore, Germany).

2.7. pH imaging

For pH imaging, zebrafish larvae (three replicates, three larvae each) were treated with 0.3, 1.3, 5, 20 and 80 ppb EZA for 3 days. The larvae were incubated with 50 μM BCECF-AM (Invitrogen, USA) for 25 min at room temperature. After washing three times with 0.3×Danieau's solution, the larvae were anesthetized in 0.001 % buffered MS-222. The fluorescence intensity was measured using a microplate reader (SpectraMax M5, Molecular Devices) with excitation at 438 nm or 513 nm and emission at 535 nm. The fluorescence intensity ratio as to 513 and 438 nm excitation was determined.

2.8. Detection of ROS

The production of ROS in zebrafish larvae was determined using membrane-permeable fluorescent dye 2',7'-dichlorodihydrofluorescin diacetate (Molecular Probes DCFH-DA; Thermo Fisher Scientific, USA) according to the method of Zeng et al. [23] with a minor modification. Three replicates of twenty larvae that had been treated with 0.3, 1.3, 5, 20 and 80 ppb EZA for 3 days were homogenized in CytoBuster protein extraction buffer (Merck, Germany). And the homogenate was centrifuged at 15,000×*g* at 4 °C for 20 min. The supernatant was incubated for 30 min with DCFH-DA in PBS (pH7.4). The fluorescence intensity was measured using a microplate reader (SpectraMax M5, Molecular Devices) with excitation and emission at 485 nm and 530 nm, respectively. The ROS levels were estimated based on a DCF (dichlorofuorescein) standard curve, and expressed as an arbitrary unit (μg DCF /mg protein) and as a percentage of a control.

2.9. Staining for mitochondrial membrane potential

For mitochondrial membrane potential staining, zebrafish larvae (three replicates, three larvae each) were treated with 80 ppb EZA for 3 days were incubated in 10 nM TMRE (tetramethylrhodamine ethyl ester perchlorate, dissolved in DMSO; Thermo Fisher Scientific, USA) for 20 min at 28.5 °C. After washing three times in 0.3×Danieau's solution, the larvae were incubated with 3 μM YO-PRO-1 for staining of hair cells

nuclei. Then samples were rinsed three times with 0.3×Danieau's solution and anesthetized with 0.001 % buffered MS-222. The labelled cells in otic neuromasts were observed under a Leika DM2500 microscope with a red fluorecence filter set for TMRE staining and a green fluorescence filter set for YO-PRO-1 staining with an Olympus DP71 camera.

2.10. Calcium imaging

For calcium imaging, zebrafish larvae (three replicates, three larvae each) were treated with 0.3, 1.3, 5, 20 and 80 ppb EZA for 3 days. The larvae were incubated with 5 μM Fura-2 AM (Dojindo Chemicals, Japan) for 30 min at room temperature, and then washed three times with 0.3×Danieau's solution. The fluorescence intensity was measured using a microplate reader (SpectraMax M5, Molecular Devices) with excitation at 340 nm or 380 nm and emission at 510 nm. The fluorescence intensity ratio as to 340 and 380 nm excitation was determined.

2.11. Cell proliferation assay

S-phase cells labeled with 5-bromo-2-deoxyuridine (BrdU) in otic neuromasts in zebrafish larvae were counted according to the method of Harris et al. [24] with a minor modification. Zebrafish larvae (three replicates, three larvae each) treated with 80 ppb EZA for 3 days were incubated in 10 mM 5-bromo-2-deoxyuridine (Sigma Aldrich, Japan) for 24 h at 28.5 °C starting at 1 h after EZA treatment. The larvae were then fixed with a 4% paraformaldehyde phosphate buffer solution (PFA) overnight at 4 °C. The fixed larvae were rinsed twice in fresh PBS and then dehydrated in a graded methanol series. Then, larvae were digested with 10 μM proteinase K (Sigma Aldrich, Japan) for 20 min, washed in PBST, and refixed in 4% PFA for 20 min. After washing twice in PBST, the larvae were incubated in 2 N HCl for 60 min at room temperature and rinsed three times in PBST. The larvae were blocked in 10 % normal goat serum for 1 h at room temperature and then incubated with the monoclonal primary anti-BrdU antibody (1:200 dilution; Santa Cruz, USA) overnight at 4 °C. After three washes, Alexa Fluor 488–conjugated secondary antibodies (Thermo Fisher Scientific, USA) were added at a dilution of 1:200 in the blocking solution, followed by incubation for 2 h at room temperature. Nuclei were labeled with 4',6-diamidino-2-phenylindole (DAPI; 1:1000 dilution; Thermo Fisher Scientific, USA) for 15 min at room temperature. Labelled cells in otic neuromasts were observed under a Leika DM2500 microscope with an Olympus DP71 camera.

2.12. Acridine orange/Ethidium bromide staining

Apoptotic cells in zebrafish larvae were labeled with Acridine orange and Ethidium bromide (Thermo Fisher Scientific, USA). Zebrafish larvae (three replicates, three larvae each) treated with 0.3, 1.3, 5, 20 and 80 ppb EZA for 3 days were incubated in 0.3×Danieau's solution containing 5 μM Acridine orange/Ethidium bromide for 20 min, rinsed three times with 0.3×Danieau's solution, and then anesthetized with 0.001 % buffered MS-222. Apoptotic cells appeared as obvious bright spots in otic vecicle were observed under a Leica DM2500 microscope with a green fluorescence filter set and an Olympus DP10 camera.

2.13. RNA isolation, cDNA synthesis and qRT-PCR

For quantitative reverse transcription-PCR (qRT-PCR) analysis, zebrafish larvae treated with 80 ppb EZA for 3 days were used. Total RNA was extracted from 3 replicates of 30–40 larvae or larvae's inner ears using Nucleo spin reagents (Takara Bio, Japan) according to the manufacturer's instructions. First strand cDNA was synthesized from 200 ng total RNA using a PrimeScript RT reagent kit (Takara Bio, Japan). The PCR was performed using SYBR premix Ex Taq II (Takara Bio, Japan) and a Takara Real-time PCR System. PCR thermal profiles comprised 45 cycles of 95 °C for 5 s and 60 °C for 30 s. The mRNA levels were expressed relative to the transcription level of the reference gene, β-actin. The relative quantification of gene expression was analyzed from the measured threshold of cycle (*CT*) using the $2^{-\Delta\Delta CT}$ method. The primers used for the analysis are listed in Table 1 and Matsumoto et al. [5].

2.14. Caspase activity

Three replicates of twenty-five larvae that had been treated with 80 ppb EZA for 3 days were washed in PBS and homogenized in cold buffer [0.32 mM sucrose, 20 mM HEPES, 1 mM $MgCl_2$, and 0.5 mM phenylmethyl sulfonylfuoride (PMSF)]. The homogenate was centrifuged at 15,000×*g* at 4 °C for 10 min, and the supernatant was assayed for caspase 3/7, 8, and 9 activities using Caspase-Glo reagents (Caspase-3/7, 8, and 9 assay system; Promega Corporation, Japan) according to the manufacturer's instructions. Luminescence was recorded with a microplate reader (SpectraMax M5, Molecular Devices). Caspase activities were expressed as percentages of the controls.

2.15. Statistical analyses

All experiments were independently repeated three to four times; all data are represented as means and standard deviations. Statistical analysis was performed using the SAS system for windows (version 9.3 TS level 1M2, SAS Institute Inc., CA, USA). Statistical comparisons were made using the two-tailed Student's *t*-test or, for multiple comparisons, one-way ANOVA followed by a Dunnet test. Values are mean ± S.D. P-value of <0.05 indicates statistical significance.

3. Results

3.1. Effect of EZA on zebrafish larval neuromast development

Our previous study demonstrated that treatment of larvae with 80 ppb (310 nM) EZA from 6 h to 5 dpf specifically inhibits otolith formation [5]. A similar tendency was also observed when treated from 6 h to 3 days post-fertilization (Fig. 1A). Then, the effect of EZA on CA activity was examined with crude extracts of larvae treated for 3 days (Fig. 1B). CA activity significantly decreased in all treated groups (treatment with 0.3, 5, 80, 310, and 1240 ppb EZA caused about 15, 25, 35, 50, and 78 % reduction of CA activity, respectively, as compared to

Table 1
Sequences of primers for the apoptosis-related genes tested.

Gene	Sequence of the primer (5'-3')	
Bax	F	GGAGGCGATACGGGCAGT
	R	TTGCGAATCACCAATGCTGTG
Bcl-2	F	TGGGCTCATCTCCTTCTCC
	R	TCTCCTCACAGCTCCACATC
Bid	F	ATGGGACAGTGGTGCAGTTTT
	R	AATCTTTCACTTCTCTAACTGCTCAACA
p53	F	GGCAATCCGAAAGTCGATAA
	R	CTGTCGTTTTGCGCCATT
Caspase-3	F	GGCAGATTTCCTCTATGCATACTC
	R	CATGAGCCGGTCATTGTG
Caspase-8	F	GATGAGAACCTGACAAGCGGTGATG
	R	GCTCATCCAGTCGCAGAATCAGGT
Caspase-9	F	AAATACATAGCAAGGCAACC
	R	CACAGGGAATCAAGAAAGG
NF-κB p65	F	AAGATGAGAACGGAGACACGC
	R	TACCAGCAATCGCAAACAACG
CHOP	F	AAGGAAAGTGCAGGAGCTGA
	R	TCACGCTCTCCACAAGAAGA
Bip	F	AAGAGGCCGAAGAGAAGGAC
	R	AGCAGCAGAAGCCTCGAAATA
β-actin	F	ATTGCTGACAGGATGCAGAAG
	R	GATGGTCCAGACTCATCGTAC TC

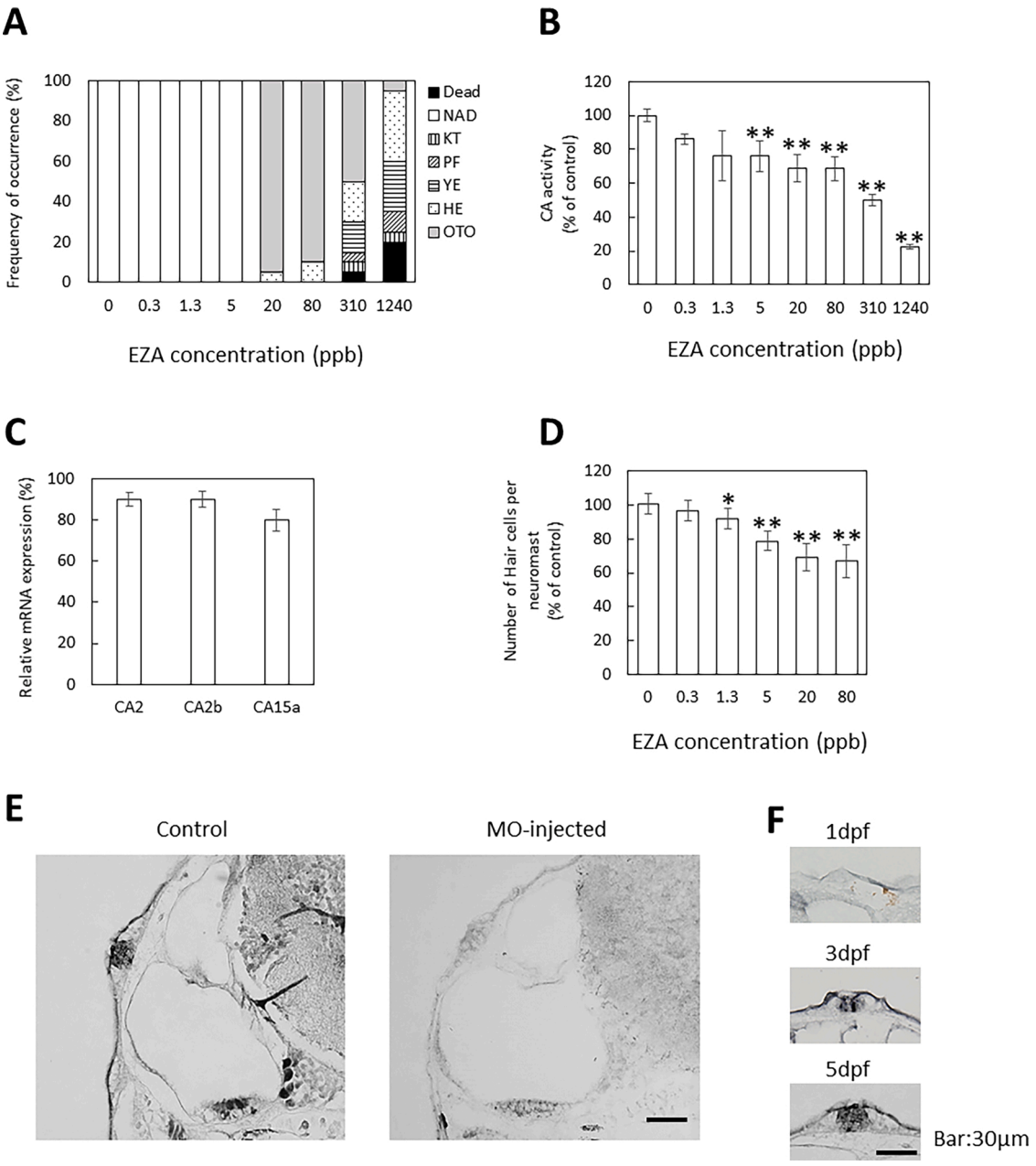

Fig. 1. Effects of EZA exposure on CA activity and otic neuromast development and location of CA in otic neuromasts. (A) Effects of EZA during zebrafish development. Analysis was performed at 3 dpf; 20 embryos were observed for each dose. The values are percentage of abnormal embryos. NAD, no abnormality detected; KT, kinked tail; PF, irregular pectoral fin; YE, Yolk edema; HE, Heart edema; OTO, small otolith. (B) Effects of EZA on CA activity. CA activity in the cytosol fraction of larvae treated with various concentrations of EZA for 3 days was measured at 3 dpf. (C) Effects of EZA on CA mRNA levels. mRNA levels of CA2, 2b and 15a in larvae treated with 80 ppb EZA for 3 days was determined at 3 dpf. The mRNA levels were measured by quantitative real-time PCR using the comparative Ct method. β-Actin was used as an internal control for normalization. (D) Effects of EZA on otic neuromast. Hair cells of otic neuromasts labeled with YO-PRO-1 after exposure to various concentrations of EZA for 3 days were counted. (E, F) Location of CA in otic neuromast. Localization of CA2 in otic neuromasts of normal zebrafish at 5 dpf (E) and 1–5 dpf (F) visualized by immunohistochemical staining. Transverse sections of otocysts in non-treated (E, F) and MO-injected (E) larvae were stained with rabbit anti-CA antiserum. The values are expressed as arbitrary units and as percentages of the control. The data are means ± SD (n = 3). Asterisks indicate significant differences from the control (ANOVA followed by Dunnet's test: *$p < 0.05$, **$p < 0.01$).

the control). This result, especially the decrease around 80 ppb, was considered to reflect the EZA amount absorbed into larvae rather than the CA concentration, since the CA expression did not seem to be affected so much by EZA treatment at 80 ppb (Fig. 1C). In further experiments, effect of up to 80 ppb of EZA on otic neuromast development was investigated, because 80 ppb (310 nM) is high enough to inhibit CA of zebrafish in vitro [the Ki of EZA for CAH-Z (CA2b in zebrafish) is 0.12 nM [25]], and EZA's specific effect was clearly observed in otolith formation at 80 ppb (Fig. 1A). For reference, LD_{50} of EZA at 5 dpf has been reported to be 9 μM [13], consistent with data in our previous study [5].

To investigate the effects of EZA treatment during neuromast development, we determined the number of hair cells in otic neuromasts of zebrafish larvae after labeling hair cell nuclei with the fluorescent dye YO-PRO-1, which specifically binds to DNA (Fig. 1D). The stained hair cells in otic neuromasts decreased in a concentration-dependent manner (8.3 ± 0.5 stained hair cells in control group, 8.0 ± 0.8 stained hair cells at 0.3 ppb, 7.5 ± 0.6 stained hair cells at 1.3 ppb, 6.5 ± 0.6 stained hair

cells at 5 ppb, 5.8 ± 1.0 stained hair cells at 20 ppb, and 5.5 ± 0.6 stained hair cells at 80 ppb).

In the previous studies, we showed the distribution of CAs in the hair cells of the inner ear epithelium during zebrafish development [5]. Since the structure and function of hair cells in the inner ear epithelium are similar to those of hair cells in neuromasts, CA was expected to be also expressed in hair cells in otic neuromasts. Actually, cytosolic enzyme CA2 was detected in hair cells of otic neuromasts, while CA2 MO-injected larvae hardly reacted with anti-CA2 antibodies (Fig. 1E). During embryogenesis, CA2 was not detected at 1 dpf, while at 3 dpf, when neuromast formation began, anti-CA2 antibodies labeled hair cells (Fig. 1F). There is a possibility that the CA that was expressed in hair cells of otic neuromasts contributed to maintenance of intracellular pH, and homeostasis of redox and ionic balance, and its inhibition by EZA treatment caused hair cell death during neuromast development.

3.2. Effects of EZA on pH and ROS level

The disruption of cellular homeostasis, including pH and ion balance, induces oxidative stress and apoptosis of hair cells [26,27]. Also, in mammals, CA inhibitor was reported to induce apoptosis by increasing the ROS level [28]. To examine the hypothesis that the increase in hair cell damage can be accounted for by pH alteration and oxidative stress, pH imaging and ROS measurement were performed. The pH alteration in zebrafish larvae was detected as changes in fluorescence intensity of a soluble pH-sensitive probe, BCECF-AM (Fig. 2A). The fluorescence ratio (513 nm/438 nm) in larvae treated with 0.3 ppb EZA for 3 days was clearly decreased as compared to in the control (Fig. 2A: 2.4 ± 0.6 in control, 1.5 ± 0.3 at 0.3 ppb, 1.2 ± 0.2 at 1.3 ppb, 0.8 ± 0.5 at 5 ppb, 0.4 ± 0.2 at 20 ppb, and 0.7 ± 0.4 at 80 ppb), indicating that CA inhibition leads to a pH decrease in larvae. The fluorescence intensity ratios in all treated groups were significantly lower than those in the control group.

The generation of ROS was detected using DCFH-DA and the level was expressed as a percentage of the control (Fig. 2B). The ROS level was significantly increased above 1.3 ppb (203 % at 0.3 ppb, 260 % at 1.3 ppb, 240 % at 5 ppb, 276 % at 20 ppb, and 266 % at 80 ppb).

3.3. Effects of EZA on mitochondrial transmembrane potential and Ca^{2+} concentration

Oxidative stress can be a trigger of mitochondrial damage such as alteration of membrane permeability, and disruption of Ca^{2+} homeostasis and the mitochondrial defense system [29]. Of these, we focused on the mitochondrial transmembrane potential, which reflects mitochondrial functionability, assessing it using the TMRE staining assay. As shown in Fig. 3, the fluorescence intensity in hair cells in otic neuromasts treated with 80 ppb EZA for 3days was clearly decreased (Fig. 3A). At this dose, zebrafish larvae showed no obvious histopathological changes in otic neuromasts.

To determine the role of Ca^{2+} in EZA-induced hair cell death, we treated zebrafish larvae with 80 ppb EZA in high calcium medium (including a 5-fold higher concentration of Ca^{2+}) (Fig. 3B). There were 5.7 ± 0.6 stained hair cells in otic neuromasts of 80 ppb EZA-treated larvae for 3 days, which was significantly lower than in the control (10.3 ± 0.6 hair cells per neuromast). With EZA treatment in high calcium medium, significantly more hair cells (9.0 ± 0.0 hair cells) remained viable, when compared to EZA treatment alone for 3 days. The number of hair cells on treatment with only high calcium medium (9.7 ± 0.6 hair cells) was comparable to that in the control even after 3 days.

Further, the calcium level in zebrafish larvae was measured as changes in fluorescence intensity of **c**alcium indicator dye, Fura-2 AM (Fig. 3C). The fluorescence ratio (340 nm/380 nm) in larvae treated with EZA for 3 days was clearly decreased as compared to in the control (1.2 ± 0.3 in control, 1.0 ± 0.1 at 0.3 ppb, 0.9 ± 0.3 at 1.3 ppb, 0.5 ± 0.04 at 5 ppb, 0.6 ± 0.3 at 20 ppb, and 0.6 ± 0.07 at 80 ppb), indicating that CA inhibition leads to a calcium level decrease in larvae.

3.4. Hair cell death in otic neuromasts is prevented by anti-oxidants

Since the ROS levels in zebrafish larvae were significantly increased by EZA (Fig. 2B), we further focused on the effects of anti-oxidants on hair cell damage in otic neuromasts (Fig. 4). Zebrafish were co-treated with EZA and GSH, allopurinol (ALO) or D-methionine (MET) as an anti-oxidant, or buthionine sulfoximine (BSO), an inhibitor of GSH synthesis, as a pro-oxidant. As shown in Fig. 4, the average number of hair cells per otic neuromast on treatment with 80 ppb EZA was clearly decreased as compared to in the control group, while co-treatment with BSO and EZA significantly enhanced the hair cell death. In contrast, co-treatment with all of the anti-oxidant agents significantly reduced the EZA-induced hair cell death. There were 9.7 ± 0.6 stained hair cells of otic neuromasts in the control group, and 6.3 ± 0.6 stained hair cells of otic neuromasts on EZA treatment for 3 days, which was in clear contrast to the anti-oxidant co-treatments. The numbers of stained hair cells of otic neuromasts in GSH and EZA, ALO and EZA, and MET and EZA for 3 days co-treated larvae were 8.7 ± 0.6, 9.0 ± 0.0, and 8.3 ± 0.6, respectively.

3.5. Effect of EZA on otic neuromast cell proliferation

Since hair cell damage in otic neuromasts was observed with EZA treatment (Fig. 1D), cell proliferation and apoptotic cells were further investigated (Fig. 5). The effect of EZA on cell proliferation in otic

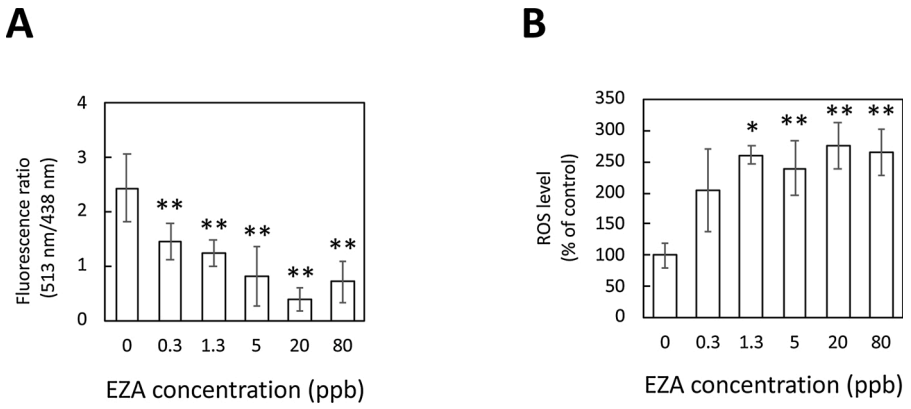

Fig. 2. pH decrease and ROS generation in larvae induced by EZA. (A) pH decrease in larvae on EZA treatment. pH changes in 3-dpf larvae treated with 0–80 ppb EZA for 3 days. (B) The ROS levels in 3-dpf larvae treated with EZA. The levels are expressed as percentages of the control. The data are means ± SD (n = 3). Asterisks indicate significant differences from the control (ANOVA followed by Dunnet's test: *p < 0.05, **p < 0.01).

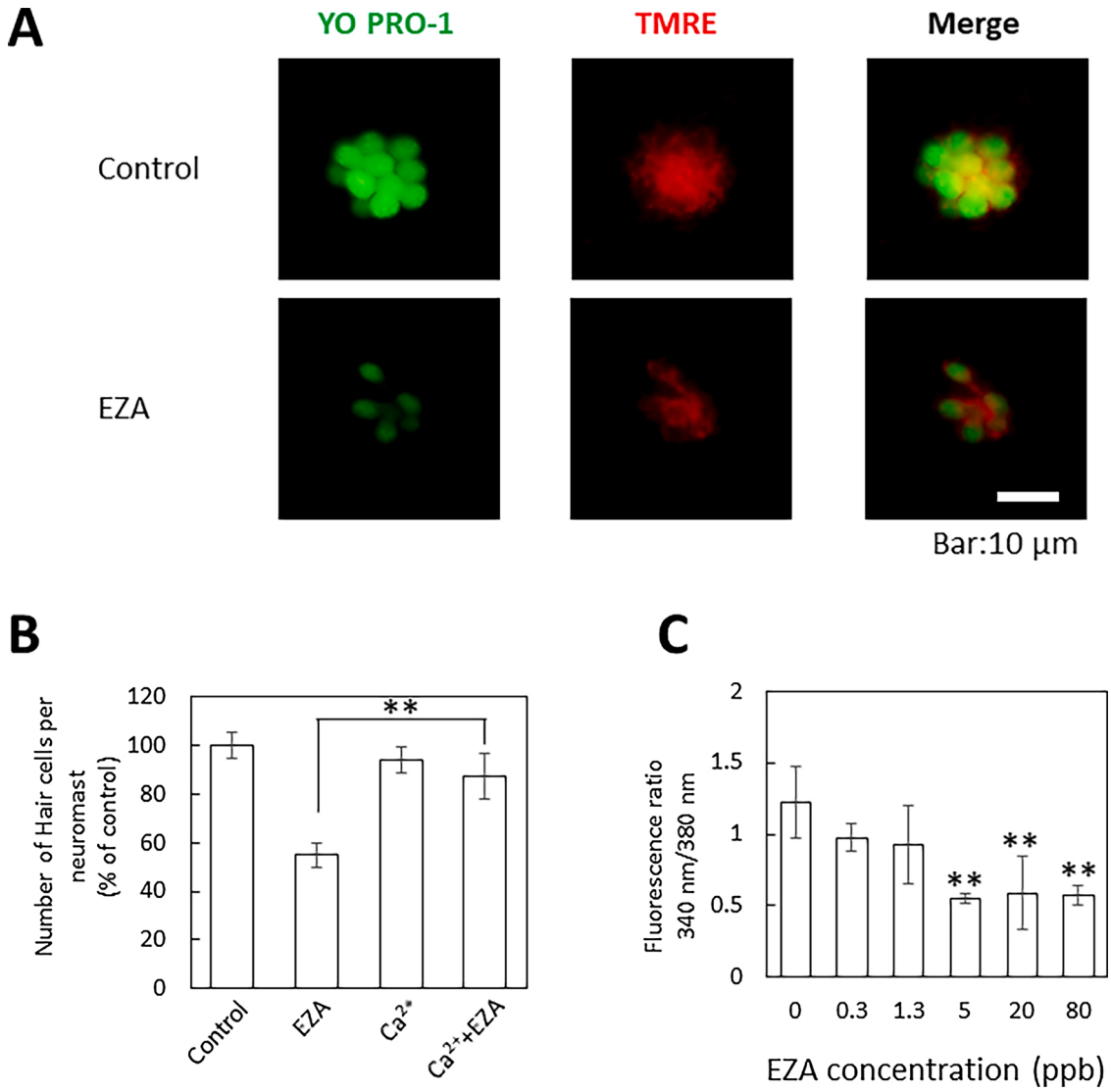

Fig. 3. Effects of EZA on mitochondrial transmembrane potential in otic neuromasts (A) and Ca^{2+} concentration in larvae (C), and relief of EZA toxicity by Ca^{2+} (B). (A) The mitochondrial transmembrane potential of otic neuromast cells in larvae (3 dpf) treated with 80 ppb EZA for 3 days was assessed by tetramethylrhodamine ethyl ester (TMRE) staining assay. (B) Zebrafish larvae (3 dpf) were treated with 80 ppb EZA in high calcium medium, and the number of hair cells in otic neuromasts was compared to that in the control and with EZA only. The levels are expressed as percentages of the control. The data are means ± SD (n = 3). Asterisks indicate significant differences from EZA (ANOVA followed by Dunnet's test: **p < 0.01). (C) The calcium levels in 3-dpf larvae treated with EZA. The data are means ± SD (n = 3). Asterisks indicate significant differences from the control (ANOVA followed by Dunnet's test: **p < 0.01).

neuromasts was examined by determining the number of S-phase cells labelled by BrdU (Fig. 5A). EZA treatment obiously reduced the number of BrdU-labeled cells, suggesting that CA inhibition causes repression of progression to the S-phase of the cell cycle in neuromasts.

Furthermore, apoptotic cells in otic vesicle was evaluated by Acridine orange/Ethidium bromide(AO/EtBr) staining (Fig. 5B). EZA treatment resulted in a concentration-dependent increase in AO/EtBr-positive cells in the otic vesicle. The numbers of AO/EtBr-positive cells treated with 1.3, 5, 20 and 80 ppb EZA for 3 days were statistically increased as compared to in the control (Fig. 5B: 1.6 ± 1.4 in control, 2.4 ± 1.1 at 0.3 ppb, 3.8 ± 1.3 at 1.3 ppb, 4.6 ± 1.3 at 5 ppb, 5.3 ± 1.0 at 20 ppb, and 8.3 ± 1.7 at 80 ppb).

3.6. Effects of EZA on mRNA expression of apoptosis-related genes and caspase activities

In a previous paper, we suggested that EZA may affect otic genesis via the apoptosis pathway [5]. Also, pH alteration and oxidative stress, which can induce apoptosis, were detected in larvae treated with EZA (Fig. 2). Thus, in this study, the expression of genes for regulation of apoptosis was analyzed to determine if the cellular death pathway is actually activated in EZA-treated larvae (Fig. 6A, B). In larvae treated with EZA, the otic mRNA expression levels of some markers for the apoptotic pathway were significantly higher than those in the control group (Fig. 6A). The level of pro-apoptotic Bax mRNA increased (1.9-fold; $p < 0.05$), while the content of anti-apoptotic Bcl-2 mRNA (1.1-fold) showed no obvious change compared to in the control group. The mRNA levels of p21, p53, CHOP, and Bip were up-regulated [2.5-fold ($p < 0.01$), 2.2-fold ($p < 0.05$), 1.3-fold, and 1.3-fold higher than in the control, when treated with 80 ppb EZA for 3 days, respectively].

The mRNA levels and activities of caspase-3 and 9, which are required for efficient execution of apoptosis, were also increased (Fig. 6A, B). The mRNA level and activity of caspase-3 on treatment with EZA showed 1.4-fold and 1.3-fold ($p < 0.05$) increases, respectively, while those of caspase-9 showed 1.3-fold and 1.2-fold increases, respectively.

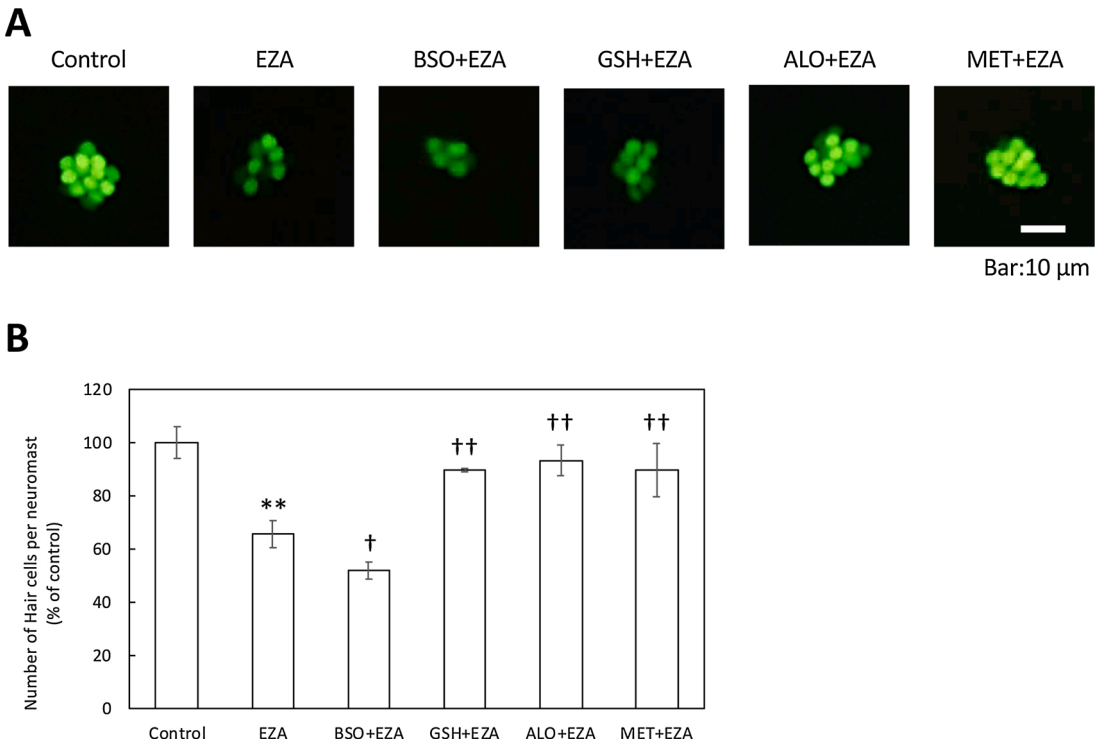

Fig. 4. Relief of EZA toxicity toward otic hair cells by anti-oxidants. Zebrafish larvae (3 dpf) were co-treated with 80 ppb EZA and glutathione (GSH), allopurinol (ALO), or D-methionine (MET) as anti-oxidants, or buthionine sulfoximine (BSO), an inhibitor of GSH synthesis, as a pro-oxidant, and then hair cells in otic neuromasts were visualized with YO-PRO-1 (A) and counted (B). The bars represent means ± SD (n = 3). Asterisks or daggers indicate significant differences from the control or EZA (Student's *t*-test, *p < 0.05 vs control, †p < 0.05 vs EZA, ††p < 0.01 vs EZA).

3.7. Inhibition of NF-κB, Bax, and p53 reduces hair cell damage by EZA

Since the mRNA expression of apoptosis-related genes and caspase activities in zebrafish larvae were significantly increased by EZA, the effects of apoptotic inhibitors on hair cell death in otic neuromasts were examined (Fig. 7). Zebrafish were treated with Bay 11-7085 or SN-50 as a NF-κB inhibitor, or 1-(3,6-dibromocarbazol-9-yl)-3-piperazin-1-yl-propan-2-ol as a Bax inhibitor, or Pifithrin-α as a p53 inhibitor, in the presence of EZA. Co-treatment with EZA and Bay 11-7085, which inhibits IkB phosphorylation, significantly repressed the level of hair cell death in otic neuromasts compared to treatment with EZA alone. Another NF-κB inhibitor, SN-50, which inhibits the nuclear translocation of NF-κB, also reduced hair cell death induced by EZA. These findings indicate that the NF-κB inhibitor reduced the EZA-induced hair cell death in otic neuromasts and that NF-κB has a pro-apoptotic effect.

Bax inhibitor 1-(3,6-dibromocarbazol-9-yl)-3-piperazin-1-yl-propan-2-ol, which inhibits Bax-mediated mitochondrial cytochrome *c* release, also reduced hair cell death in otic neuromasts induced by EZA. Co-treatment with EZA and pifithrin-α, which inhibits p53 binding to mitochondria by reducing its affinity to antiapoptotic proteins Bcl-xL and Bcl-2, almost completely inhibited hair cell death in otic neuromasts caused by EZA.

The numbers of stained hair cells of otic neuromasts in control, EZA, Bay 11-7085 and EZA, SN-50 and EZA, Bax inhibitor and EZA, and Pif-α and EZA for 3 days co-treated larvae were 10.3 ± 0.6, 5.7 ± 0.6, 7.6 ± 0.6, 8.3 ± 0.6, 8.3 ± 0.6, and 10.0 ± 0.0, respectively.

4. Discussion

EZA inhibited CA activity, decreased pH, and increased the ROS levels in larvae, and remarkably induced hair cell death in neuromasts (Figs. 1 and 2). In neuromast hair cells, cytosolic CA2 was expressed during embryogenesis (Fig. 1). These findings suggest that CAs including CA2 are required for neuromast hair cell development. Furthermore, the relationship between ROS production and hair cell death in otic neuromasts was examined, since ROS production can be a trigger of hair cell death. EZA-induced hair cell death was prevented by anti-oxidants, suggesting that EZA negatively affects cell proliferation via increased production of ROS (Figs. 2 and 4). Then, the expression of intrinsic apoptosis genes that are known to be induced by ROS was analyzed to determine if activation of the apoptotic signaling pathway was caused by EZA. The mRNA levels of Bax, p53, NF-κB, and caspase-3 and -9, which are involved in intrinsic apoptosis and cell proliferation, were increased (Fig. 6).

Apoptotic inhibitors, Bax, p53, and NF-κB inhibitors, significantly inhibited hair cell death, demonstrating that these target proteins are involved in apoptosis caused by EZA (Fig. 7). These findings indicate that EZA induces apoptosis through an intrinsic pathway.

In a previous study, CA2 and CA15a were shown to be expressed in hair cells and transitional cells in the inner ear epithelium at the beginning of embryogenesis [5], and to be important for organ formation. Since inner ear hair cells are morphologically and functionally very similar to neuromast hair cells [30,31], CA in both types of cells was expected to play a similar role in the development of the organs. CA in epithelium cells and the hair bundle of the inner ear plays a central role in the transport of calcium, protons, and bicarbonate ions. Also, CA can regulate the activities of anion exchangers or Na^+-HCO_3^- cotransporters by being associated with them [32,33]. Lin [20] showed that anion exchanger 1 (AE1), which is a bicarbonate transporter, was expressed in stereocilia of neuromast hair cells, and hypothesized that AE1 might form a multiprotein complex with other proteins such as CA, to regulate ion and acid-base balance in the hair bundle. Our results regarding localization of CA in the neuromast (Figs. 1 and 2) support their hypothesis, although the exact function of CA and the formation of a multiprotein complex in neuromast hair cells remain unclear. Moreover, other reports describe that deletion of Cl^-/HCO_3^- exchanger and treatment with H^+-ATPase inhibitors lead to acidification of the endolymph [34–36], and that pH alteration decreases the hair cell number and

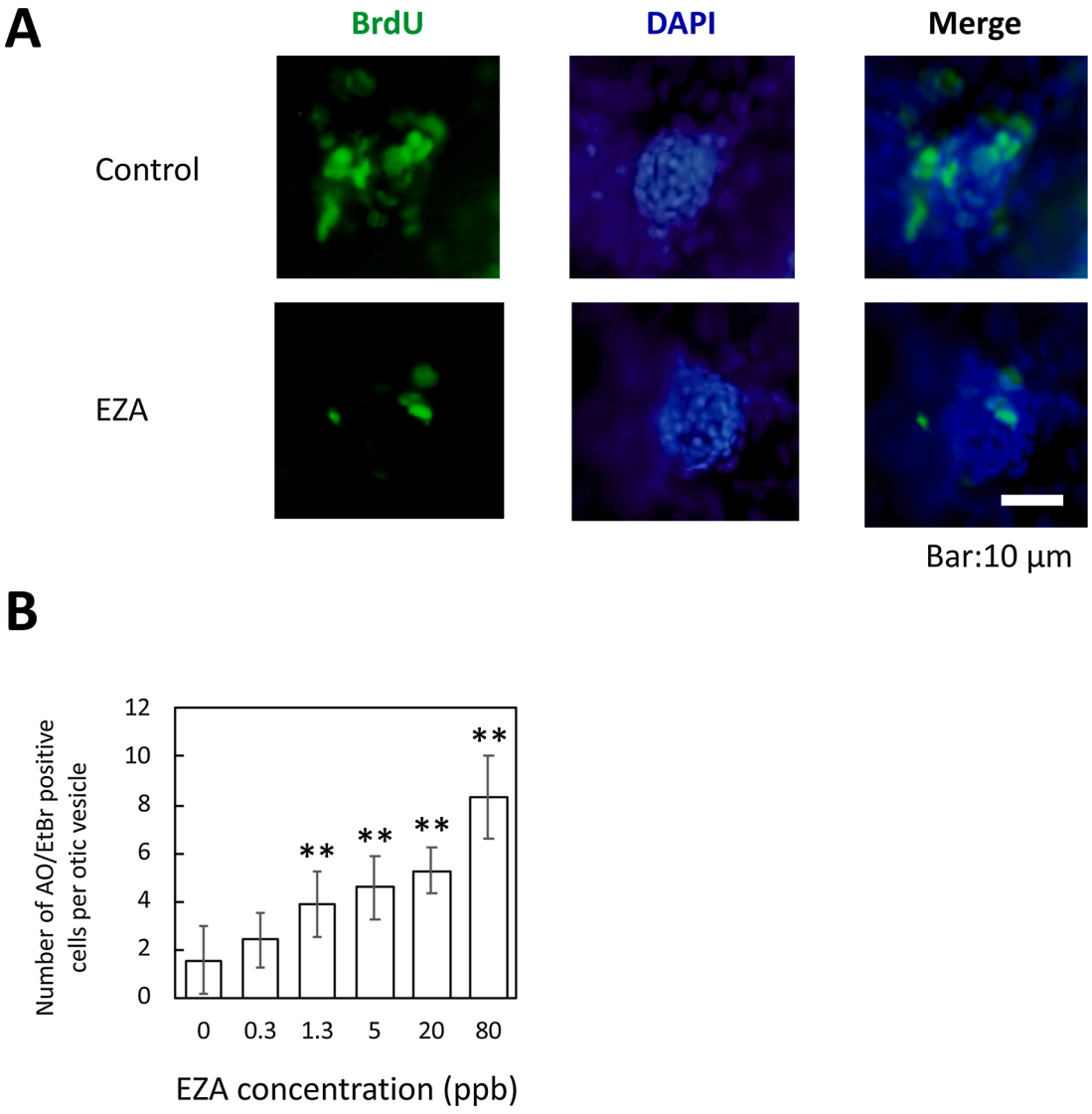

Fig. 5. Effect of EZA on otic neuromast cell proliferation and apoptotic cells in otic vesicle. (A) Repression of progression to the S-phase of the cell cycle by EZA. DNA-replicating cells were labeled with BrdU. (B) Apoptosis of cells in the otic vesicle. Apoptotic cells were detected by Acridine orange/Ethidium bromide, and were counted and plotted as mean ± SD (n = 3). Asterisks indicate significant differences from the control (ANOVA followed by Dunnet's test: **p < 0.01).

function [37,38]. Thus, CA and other transporters are considered to play important roles in maintaining pH and ion homeostasis in the neuromast development. Acidification of the external environment around hair cells can also cause decreased Ca^{2+} entry into hair cells through Ca^{2+} channels [39,40].

Since EZA decreased calcium level in larvae and hair cell death was rescued by the addition of calcium, it was suggested that cellular acidification may suppress Ca influx in hair cell. Fish raised in an acidic environment or ones with knocked down H^+-ATPase or Cl^-/HCO_3^- exchanger show decreased Ca^{2+} levels and hair cell death [37,38,41,42]. These data suggesting that inhibition of ion transport induces disruption of cellular Ca^{2+} homeostasis and/or pH balance, ultimately leading to apoptosis, are consistent with our idea based on the results in this study.

ROS production can be a trigger of mitochondrial membrane damage and hair cell death, which cause the perturbation of cellular Ca^{2+} homeostasis, such as cytosolic Ca^{2+} overload, endoplasmic reticulum (ER) Ca^{2+} depletion, and mitochondrial Ca^{2+} increase.

Cellular acidification has been reported to be related to an increase in the cellular level of ROS and also promotes apoptosis by favoring caspase-3 activation [33,43]. The increased amount of ROS induces mitochondria damage and activation of the intrinsic apoptotic pathway. In this study, EZA decreased the mitochondrial membrane potential and anti-oxidants reduced hair cell death, indicating that EZA induces apoptosis via ROS generation. Furthermore, we revealed the molecular pathway underlying the hair cell death via up-regulation of apoptotic protein and subsequent caspase activation.

There are multiple possible mechanisms by which ROS production could lead to defects in hair cell function. Recent studies showed that ROS overproduction, an abnormal cellular pH, and redox disruption lead to endoplasmic reticulum (ER) stress [44], and that ER stress induces hair cell apoptosis [45,46]. In our study, the mRNA levels of Bip and CHOP, which are induced in response to ER stress, which is defined as the accumulation of unfolded or misfolded protein in ER, were increased. p53 is also a relevant mediator of ER stress–dependent apoptosis through the transcriptional upregulation. All of ROS production, alteration of cellular pH, and redox disruption induced by EZA can lead to ER stress. Further experiments are required to examine ER stress inducers.

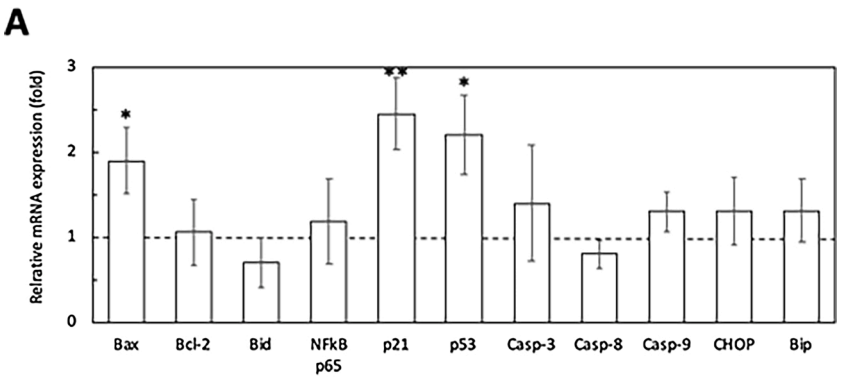

Fig. 6. Effects of EZA treatment on expression of genes for the apoptotic pathway (A) and caspase activities (B). The otic mRNA expression levels of some markers for the apoptotic pathway (A) and caspase activities (B) in inner ears isolated from EZA-treated zebrafish larvae (3 dpf) were determined. The EZA treatment was performed at 80 ppb for 3 days. The mRNA levels were measured by quantitative real-time PCR using the comparative Ct method. β-Actin was used as an internal control for normalization. The bars represent means ± SD (n = 3) (Student's *t*-test, *p < 0.05, **p < 0.01).

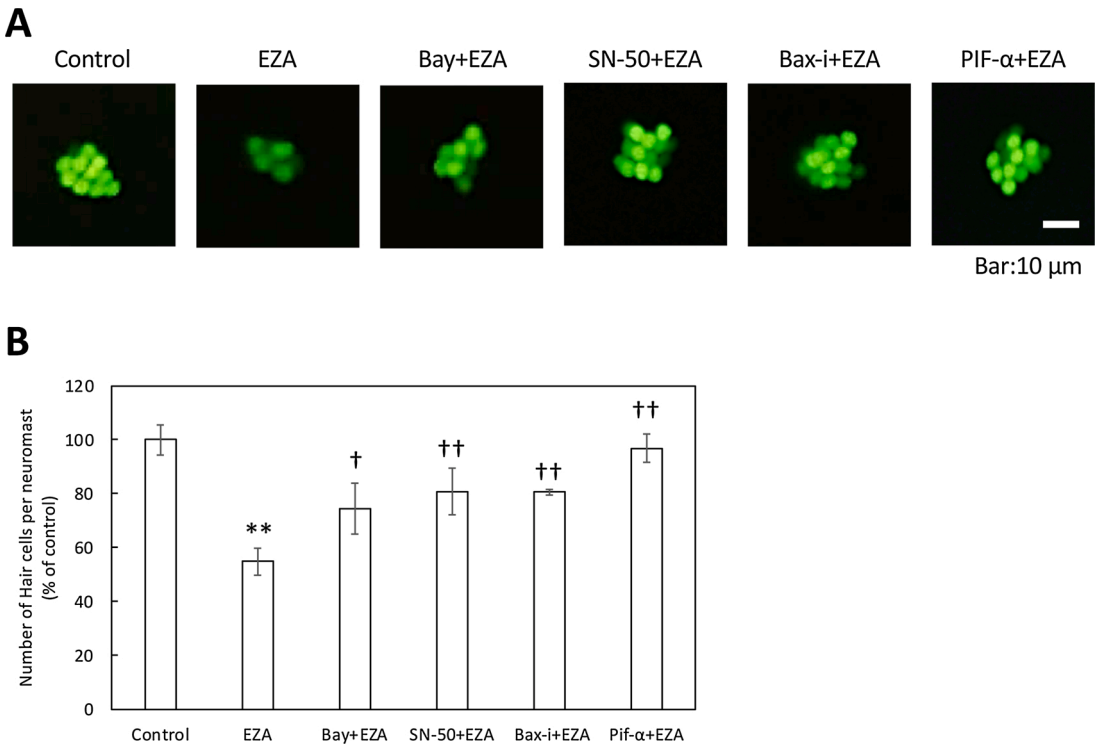

Fig. 7. Relief of EZA toxicity toward otic hair cells by apoptotic inhibitors. Zebrafish larvae (3 dpf) were treated with Bay 11-7085 (Bay) or SN-50 as NF-κB inhibitors, or Bax inhibitor (Bax-i), or PIF-α as a p53 inhibitor, in the presence of EZA at 80 ppb for 3 days, and then hair cells in otic neuromasts were visualized with YO-PRO-1 (A) and counted (B). The bars represent means ± SD (n = 3). Asterisks or daggers indicate significant differences from the control or EZA (Student's *t*-test, *p < 0.05 vs control, †p < 0.05 vs EZA, ††p < 0.01 vs EZA).

5. Conclusion

In summary, EZA-induced hair cell death was obvious, especially in neuromast development. Our results indicate that the molecular mechanism regulating the EZA-induced hair cell death is mediated by an intrinsic apoptotic pathway. CA, which plays an important role in neuromast development, is directly exposed to chemicals in the ambient environment, and shows marked sensitivity to these chemicals, especially in immature fish. Our results demonstrated that CA activity is essential for maintenance of ion transport during the development of

neuromasts in the zebrafish lateral line.

Authors contributions

H.M. and S.F. designed the experiments; H.M., H.M, and Y.S. conducted the experiments; H.M. analyzed the data; H.M. and S.F. wrote the manuscript. All authors edited and approved the manuscript.

Funding

This work was supported by JSPS KAKENHI Grant Numbers JP16K07427 and JP20K06326, and the Promotion and Mutual Aid Corporation for Private Schools.

Conflict of interest

The authors declare no conflict of interest.

Declaration of Competing Interest

The authors report no declarations of interest.

Acknowledgements

The authors are indebted to Mr. N. J. Halewood for correcting the English version of this paper.

Appendix A. Supplementary data

Supplementary material related to this article can be found, in the online version, at doi:https://doi.org/10.1016/j.toxrep.2021.11.018.

References

[1] K.M. Gilmour, New insights into the many functions of carbonic anhydrase in fish gills, Respir. Physiol. Neurobiol. 184 (2012) 223–230.
[2] L. Wu, B. Sagong, J.Y. Choi, U.K. Kim, J. Bok, A systematic survey of carbonic anhydrase mRNA expression during mammalian inner ear development, Dev. Dyn. 242 (2013) 269–280.
[3] M.G. Lionetto, R. Caricato, M.E. Giordano, E. Erroi, T. Schettino, Carbonic anhydrase as pollution biomarker: an ancient enzyme with a new use, Int. J. Environ. Res. Public Health 9 (2012) 3965–3977.
[4] M.G. Lionetto, R. Caricato, M.E. Giordano, Carbonic anhydrase sensitivity to pesticides: perspectives for biomarker development, Int. J. Mol. Sci. 21 (2020) 3562.
[5] H. Matsumoto, S. Fujiwara, H. Miyagi, N. Nakamura, Y. Shiga, T. Ohta, M. Tsuzuki, Carbonic anhydrase inhibitors induce developmental toxicity during zebrafish embryogenesis, especially in the inner ear, Mar. Biotechnol. 19 (2017) 430–440.
[6] A. Topal, A. Atamanalp, E. Oruc, Y. Demir, S. Beydemir, A. Isil, In vivo changes in carbonic anhydrase activity and histopathology of gill and liver tissues after acute exposure to chlorpyrifos in rainbow trout, Arh. Hig. Rada Toksikol. 65 (2014) 377–385.
[7] S. Doğan, The in vitro effects of some pesticides on carbonic anhydrase activity of *Oncorhynchus mykiss* and *Cyprinus carpio* fish, J. Hazard. Mater. 132 (2006) 171–176.
[8] M. del Pilar Corena, P. van den Hurk, H. Zhong, C. Brock, R. Mowery, J.V. Johnson, P.J. Linser, Degradation and effects of the potential mosquito larvicides methazolamide and acetazolamide in sheepshead minnow (*Cyprinodon variegatus*), Ecotoxicol. Environ. Saf. 64 (2006) 369–376.
[9] R. Demirdağ, E. Yerlikaya, E. Aksakal, Ö.I. Küfrevioğlu, D. Ekinci, Influence of pesticides on the pH regulatory enzyme, carbonic anhydrase, from European Seabass liver and bovine erythrocytes, Environ. Toxicol. Pharmacol. 34 (2012) 218–222.
[10] E.D. Kaya, H. Söyüt, Ş. Beydemir, Carbonic anhydrase activity from the gilthead sea bream (*Sparus aurata*) liver: The toxicological effects of heavy metals, Environ. Toxicol. Pharmacol. 36 (2013) 514–521.
[11] D. Daniel, G.D. de Alkimin, B. Nunes, Single and combined effects of the drugs salicylic acid and acetazolamide: Adverse changes in physiological parameters of the freshwater macrophyte, *Lemna gibba*, Environ. Toxicol. Pharmacol. 79 (2020), 103431.
[12] G. Streisinger, C. Walker, N. Dower, D. Knauber, F. Singer, Production of clones of homozygous diploid zebra fish (*Brachydanio rerio*), Nature 291 (1981) 293–296.
[13] J. Kazokaitė, A. Aspatwar, V. Kairys, S. Parkkila, D. Matulis, Fluorinated benzenesulfonamide anticancer inhibitors of carbonic anhydrase IX exhibit lower toxic effects on zebrafish embryonic development than ethoxzolamide, Drug Chem. Toxicol. 40 (2017) 309–319.
[14] A. Aspatwar, H.M. Becker, N.K. Parvathaneni, M. Hammaren, A. Svorjova, H. Barker, C.T. Supuran, L. Dubois, P. Lambin, M. Parikka, S. Parkkila, J.Y. Winum, Nitroimidazole-based inhibitors DTP338 and DTP348 are safe for zebrafish embryos and efficiently inhibit the activity of human CA IX in *Xenopus oocytes*, J. Enzyme Inhib. Med. Chem. 33 (2018) 1064–1073.
[15] A. Aspatwar, M. Hammaren, M. Parikka, S. Parkkila, F. Carta, M. Bozdag, D. Vullo, C.T. Supuran, In vitro inhibition of *Mycobacterium tuberculosis* beta-carbonic anhydrase 3 with Mono- and dithiocarbamates and evaluation of their toxicity using zebrafish developing embryos, J. Enzyme Inhib. Med. Chem. 35 (2020) 65–71.
[16] T.Y. Lin, B. Liao, J. Horng, J. Yan, C. Hsiao, P. Hwang, Carbonic anhydrase 2-like a and 15a are involved in acid-base regulation and Na^+ uptake in zebrafish H^+-ATPase-rich cells, Am. J. Physiol. Cell Physiol. 294 (2008) C1250–C1260.
[17] G.Y. Hung, C.L. Wu, Y.L. Chou, C.T. Chien, J.L. Horng, L.Y. Lin, Cisplatin exposure impairs ionocytes and hair cells in the skin of zebrafish embryos, Aquat. Toxicol. 209 (2019) 168–177.
[18] M. Beier, R. Hilbig, R. Anken, Histochemical localisation of carbonic anhydrase in the inner ear of developing cichlid fish, *Oreochromis mossambicus*, Adv. Space Res. 42 (2008) 1986–1994.
[19] H. Tohse, E. Murayama, T. Ohira, Y. Takagi, H. Nagasawa, Localization and diurnal variations of carbonic anhydrase mRNA expression in the inner ear of the rainbow trout *Oncorhynchus mykiss*, Comp. Biochem. Physiol. B 145 (2006) 257–264.
[20] L.Y. Lin, G.Y. Hung, L.C. Wu, S.W. Chen, L.Y. Lin, J.L. Horng, Anion exchanger 1b in stereocilia is required for the functioning of mechanotransducer channels in lateral-line hair cells of zebrafish, PLoS One 10 (2015), e0117041.
[21] A.L. Gustafson, D.B. Stedman, J. Ball, J.M. Hillegass, A. Flood, C.X. Zhang, J. Panzica-Kelly, J. Cao, A. Coburn, B.P. Enright, M.B. Tornesi, M. Hetheridge, K. A. Augustine-Rauch, Inter-laboratory assessment of a harmonized zebrafish developmental toxicology assay – Progress report on phase I, Reprod. Toxicol. 33 (2012) 155–164.
[22] Y. Ito, S. Kobayashi, N. Nakamura, H. Miyagi, M. Esaki, K. Hoshijima, S. Hirose, Close association of carbonic anhydrase (CA2a and CA15a), Na^+/H^+ exchanger (Nhe3b), and ammonia transporter Rhcg1 in zebrafish ionocytes responsible for Na^+ uptake, Front. Phys. 4 (2013) 59.
[23] C. Zeng, H. Sun, P. Xie, J. Wang, G. Zhang, N. Chen, W. Yan, G. Li, The role of apoptosis in MCLR-induced developmental toxicity in zebrafish embryos, Aquat. Toxicol. 149 (2014) 25–32.
[24] J.A. Harris, A.G. Cheng, L.L. Cunningham, G. MacDonald, D.W. Raible, E.W. Rubel, Neomycin-induced hair cell death and rapid regeneration in the lateral line of zebrafish (*Danio rerio*), J. Assoc. Res. Otolaryngol. 4 (2003) 219–234.
[25] R.E. Peterson, C. Tu, P.J. Linser, Isolation and characterization of a carbonic anhydrase homologue from the zebrafish (*Danio rerio*), J. Mol. Evol. 44 (1997) 432–439.
[26] S. Morrill, D.Z. He, Apoptosis in inner ear sensory hair cells, J. Otol. 12 (2017) 151–164.
[27] R. Esterberg, T. Linbo, S.B. Pickett, P. Wu, H.C. Ou, E.W. Rubel, D.W. Raible, Mitochondrial calcium uptake underlies ROS generation during aminoglycoside-induced hair cell death, J. Clin. Invest. 126 (2016) 3556–3566.
[28] K. Al-Khayal, A. Alafeefy, M.A. Vaali-Mohammed, A. Mahmood, A. Zubaidi, O. Al-Obeed, Z. Khan, M. Abdulla, R. Ahmad, Novel derivative of aminobenzenesulfonamide (3c) induces apoptosis in colorectal cancer cells through ROS generation and inhibits cell migration, BMC Cancer 17 (2017) 4.
[29] C. Guo, L. Sun, X. Chen, D. Zhang, Oxidative stress, mitochondrial damage and neurodegenerative diseases, Neural Regen. Res. 8 (2013) 2003–2014.
[30] T.T. Whitfield, Zebrafish as a model for hearing and deafness, J. Neurobiol. 53 (2002) 157–171.
[31] T. Nicolson, The genetics of hearing and balance in zebrafish, Annu. Rev. Genet. 39 (2005) 9–22, https://doi.org/10.1146/annurev.genet.39.073003.105049.
[32] D. Lee, J.H. Hong, The fundamental role of bicarbonate transporters and associated carbonic anhydrase enzymes in maintaining ion and pH homeostasis in non-secretory organs, Int. J. Mol. Sci. 21 (2020) 339.
[33] E.M. Kniep, C. Roehlecke, N. Ozkucur, A. Steinberg, F. Reber, L. Knels, R.H. Funk, Inhibition of apoptosis and reduction of intracellular pH decrease in retinal neural cell cultures by a blocker of carbonic anhydrase, Invest. Ophthalmol. Vis. Sci. 47 (2006) 1185–1192.
[34] P. Wangemann, K. Nakaya, T. Wu, R.J. Maganti, E.M. Itza, J.D. Sanneman, D. G. Harbidge, S. Billings, D.C. Marcus, Loss of cochlear HCO_3^- secretion causes deafness via endolymphatic acidification and inhibition of Ca^{2+} reabsorption in a Pendred syndrome mouse model, Am. J. Physiol. Renal Physiol. 292 (2007) F1345–F1353.
[35] V. Couloigner, M. Teixeira, P. Hulin, O. Sterkers, M. Bichara, B. Escoubet, G. Planelles, Effect of locally applied drugs on the pH of luminal fluid in the endolymphatic sac of guinea pig, Am. J. Physiol. Regul. Integr. Comp. Physiol. 279 (2000) R1695–R1700.
[36] O. Sterkers, G. Saumon, P. Tran Ba Huy, E. Ferrary, C. Amiel, Electrochemical heterogeneity of the cochlear endolymph: effect of acetazolamide, Am. J. Physiol. 246 (1984) F47–F53.
[37] L.Y. Lin, G.Y. Hung, Y.H. Yeh, S.W. Chen, J.L. Horng, Acidified water impairs the lateral line system of zebrafish embryos, Aquat. Toxicol. (2019), 105351.
[38] T.M. Stawicki, K.N. Owens, T. Linbo, K.E. Reinhart, E.W. Rubel, D.W. Raible, The zebrafish merovingian mutant reveals a role for pH regulation in hair cell toxicity and function, Dis. Model. Mech. 7 (2014) 847–856.
[39] K. Ikeda, Y. Saito, A. Nishiyama, T. Takasaka, Effects of pH on intracellular calcium levels in isolated cochlear outer hair cells of guinea pigs, Am. J. Physiol. Cell Physiol. 261 (1991) C231–C236.

[40] C.T. Tan, S.Y. Lee, C.J. Yao, S.H. Liu, S.Y. Lin-Shiau, Effects of gentamicin and pH on [Ca^{2+}] in apical and basal outer hair cells from guinea pigs, Hear. Res. 154 (2001) 81–87.
[41] J.L. Horng, L.Y. Lin, C.J. Huang, F. Katoh, T. Kaneko, P.P. Hwang, Knockdown of V-ATPase subunit A (atp6v1a) impairs acid secretion and ion balance in zebrafish (*Danio rerio*), Am. J. Physiol. Regul. Integr. Comp. Physiol. 292 (2007) R2068–R2076.
[42] J.L. Horng, L.Y. Lin, P.P. Hwang, Functional regulation of H^+-ATPase-rich cells in zebrafish embryos acclimated to an acidic environment, Am. J. Physiol. Cell Physiol. 296 (2009) C682–C692.
[43] T.F. Sergeeva, M.V. Shirmanova, O.A. Zlobovskaya, A.I. Gavrina, V.V. Dudenkova, M.M. Lukina, K.A. Lukyanov, E.V. Zagaynova, Relationship between intracellular pH, metabolic co-factors and caspase-3 activation in cancer cells during apoptosis, Biochim. Biophys. Acta Mol. Cell Res. 1864 (2017) 604–611.
[44] M. Seervi, A. Rani, A.K. Sharma, T.R. Santhosh Kumar, ROS mediated ER stress induces Bax-Bak dependent and independent apoptosis in response to Thioridazine, Biomed. Pharmacother. 106 (2018) 200–209.
[45] Y. Wang, Z. Xu, Endoplasmic reticulum stress as target for treatment of hearing loss, STEMedicine 1 (2020) e21.
[46] S. Oyadomari, M. Mori, Roles of CHOP/GADD153 in endoplasmic reticulum stress, Cell Death Differ. 11 (2004) 381–389.